Electronic Supplementary Material (ESI) for Journal of Materials Chemistry A.

Supporting Information

Experimental Section

Synthesis of TiO_2 nanoparticles. 2 mL $TiCl_4$ was firstly added dropwise to 8 mL ethanol under vigorous stirring. The resulting solution was then added to 40 mL benzyl alcohol also under stirring, followed by reaction at 80 ^{o}C for 9 h. The produced translucent solution was cooled down to room temperature and thus mixed with diethyl ether to obtain TiO_2 nanoparticle precipitant. The TiO_2 precipitant was centrifuged and washed with acetone for three times. The dried TiO_2 nanoparticles were re-dispersed in ethanol at a concentration of 9 mg/mL with 20 mol% titanium diisopropoxide bis(acetylacetonate). After standing still for several hours, a stable and translucent precursor solution was obtained.

Synthesis of CH_3NH_3I. Hydroiodic acid aqueous solution (45 wt%, 12.5 mL) was added dropwise to a methylamine solution (6.4 wt%, 124 mL ethanol) at 0 ^{o}C under stirring and kept for 2 h in dark. The resulting solution was treated by a rotatory evaporator at 50 °C and then re-crystallized with hot ethanol, followed by precipitation with diethyl ether for 3 times to produce a white powder of methylamine iodide. After drying in a vacuum condition, the powder was kept in dark and dried prior to the use.

Synthesis of aligned carbon nanotube array and sheet. The spinnable carbon nanotube (CNT) array was synthesized by chemical vapor deposition in a 1-inch furnace. The sequential two layers with 1.2 nm Fe and 5 nm Al_2O_3 were used as the catalyst. Ethylene with a flowing rate of 45 sccm was used as carbon precursor, and a mixture of 15 sccm hydrogen plus 200 sccm argon served as carrier gas. A CNT array with a height of 300 μm was obtained after growth for 12 min at 740 ^{o}C. The CNT sheet was dry-drawn from the CNT array.

Transient and steady state spectroscopy measurements. The samples were prepared on glass substrate. All measurements were conducted in an optical cryostat under vacuum at room temperature. For transient absorption spectroscopy, a Ti:Sapphire amplifier laser with wavelength of 800 nm was used. The pulse width and the repetition rate were 120 fs and 1 kHz respectively. The pump pulses at 400 nm were obtained by doubling the amplifier's fundamental output with a BBO crystal. The pump beam at a fluence of

70 μJ/cm^2 was modulated by a mechanical chopper at ~320 Hz. We focused on the sample with a spot diameter of ~3 mm. The fundamental 800 nm light was focused into a sapphire plate to generate the supercontinuum white light, which passed through a filter with the central transmission wavelength of 950 nm and the bandwidth of 10 nm to serve as the probe pulse. The pump and probe beam were spatially overlapped on the sample, and the probe light showed a much lower energy density than the pump beam. The transmitted probe pulse was detected by a silicon photodiode connected to a lock-in amplifier. For the steady state photoluminescence spectroscopy, a semiconductor laser with the wavelength of 447 nm, modulated by a chopper at the frequency of 325 Hz, was used as the pump beam. The wavelength of the photoluminescence was selected by a monochrometer, and a long pass filter (>500 nm) was placed before the monochrometer to eliminate the influence of the stray light of the pump beam. The detection of the photoluminescence signal was achieved by a Si photodetector combined with a lock-in amplifier.

Characterization. The structures were measured by scanning electron microscopy (Hitachi FE-SEM S-4800 operated at 1 kV). X-ray diffraction patterns were obtained from an X-ray powder diffractometer (D8 ADVANCE and DAVINCI.DESIGN). The thicknesses were obtained from a surface profiler (Veeco, Dektak 150). J-V curves were recorded from a Keithley 2420 Source Meter under illumination (100 mW/cm^2) of simulated AM1.5 solar light coming from a solar simulator (Oriel-Sol3A 94023A equipped with a 450 W Xe lamp and an AM1.5 filter). The light intensity was calibrated using a reference Si solar cell (Oriel-91150).

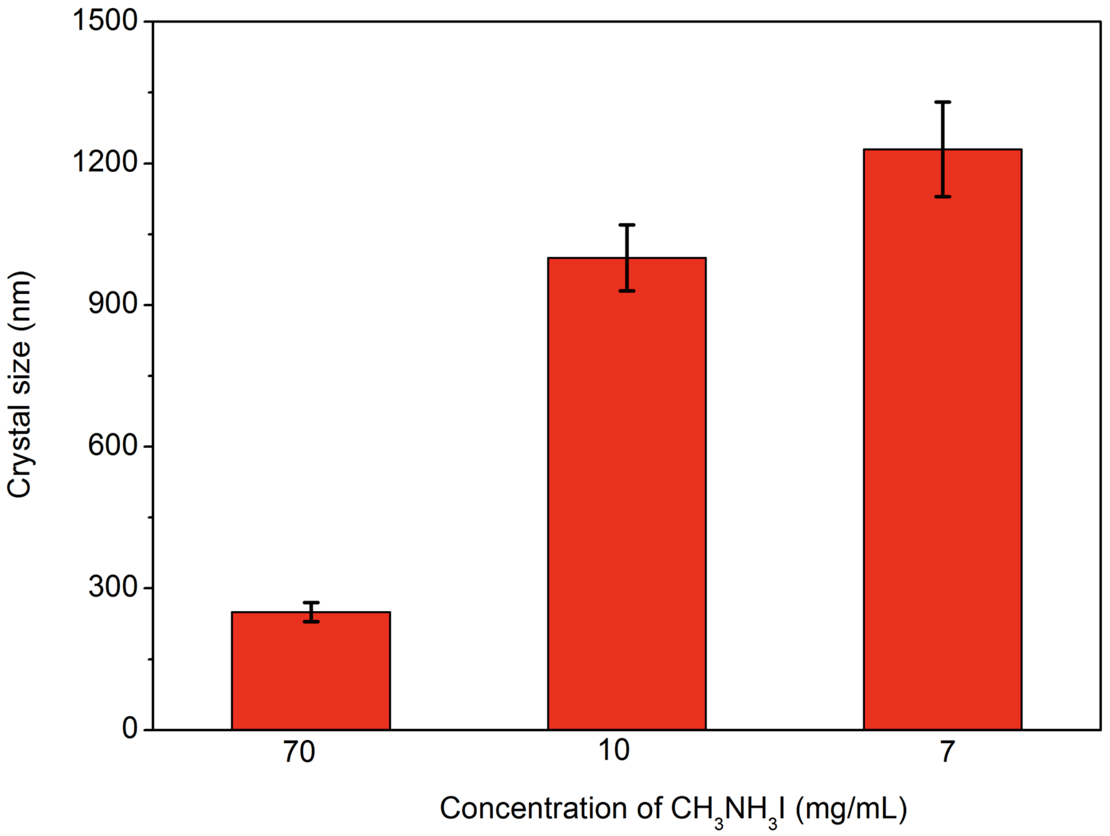

Figure S1. Dependence of the size of $CH_3NH_3PbI_3$ crystal on the concentration of CH_3NH_3I solution.

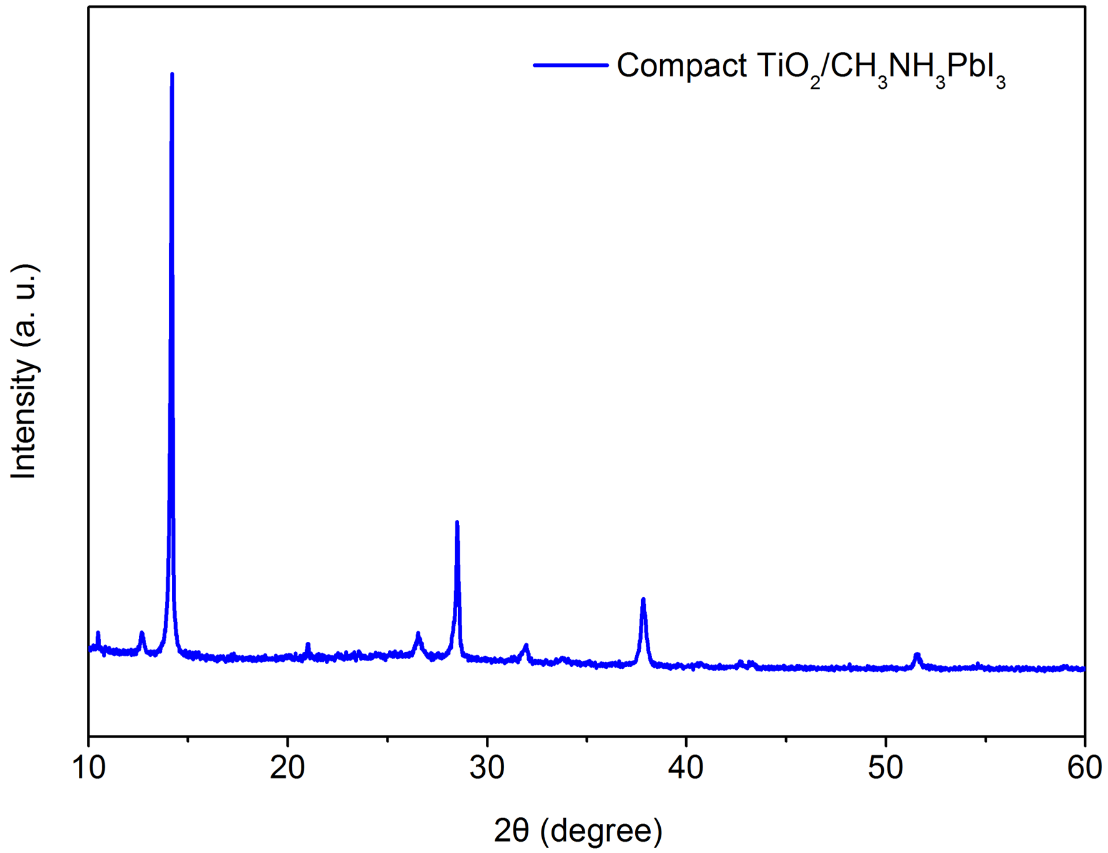

Figure S2. X-ray diffraction pattern of the perovskite layer with crystal size of ~1 μm.

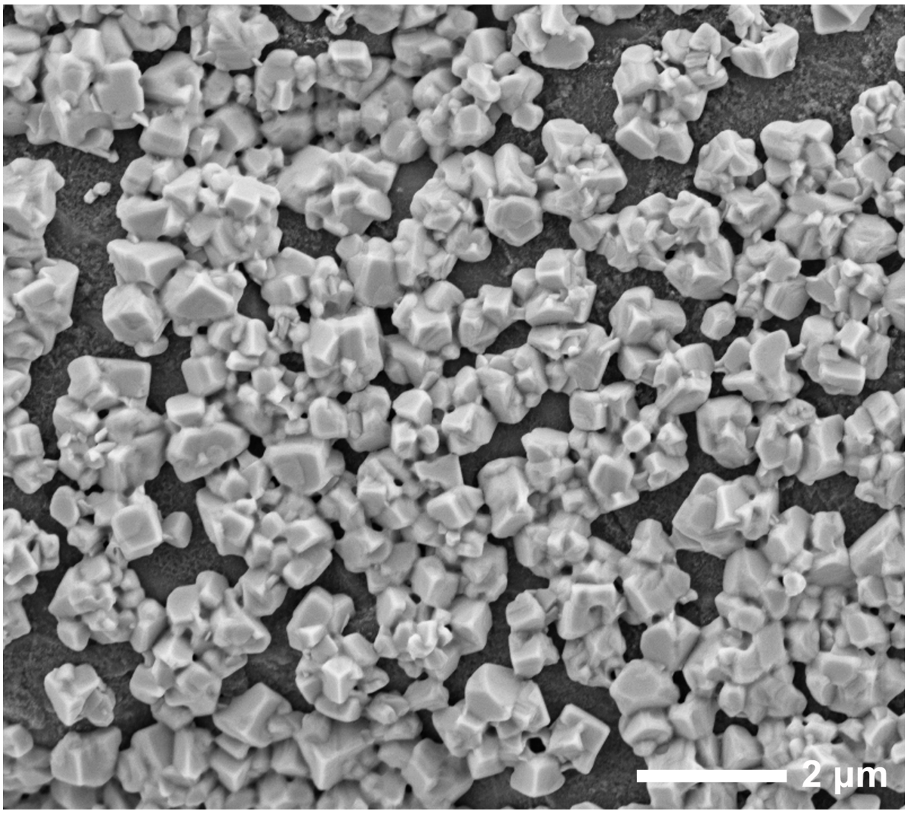

Figure S3. Scanning electron microscopy (SEM) image of $CH_3NH_3PbI_3$ crystals coated on a curved fiber surface.

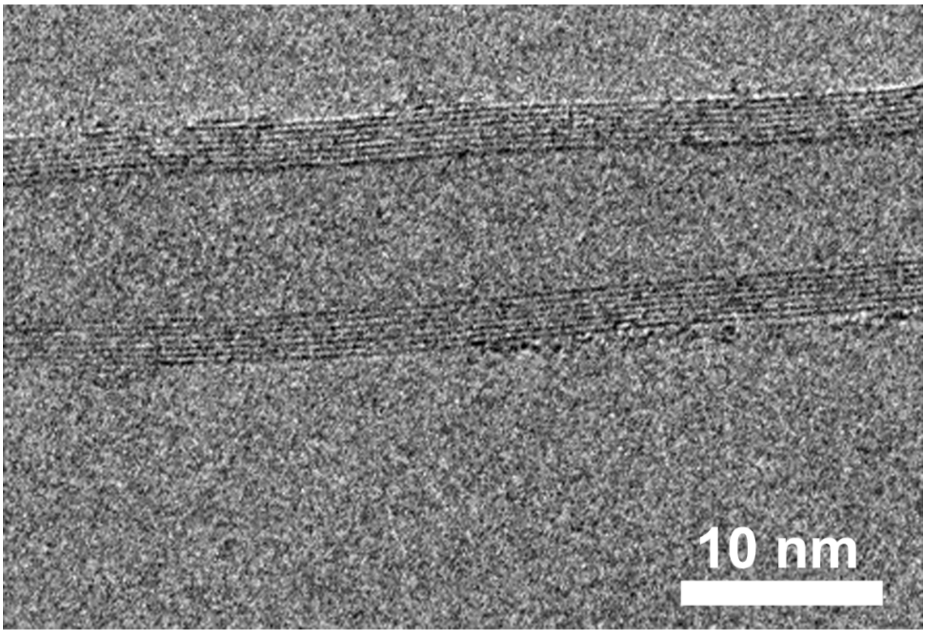

Figure S4. High-resolution transmission electron microscopy image of a CNT with the diameter of ~12 nm.

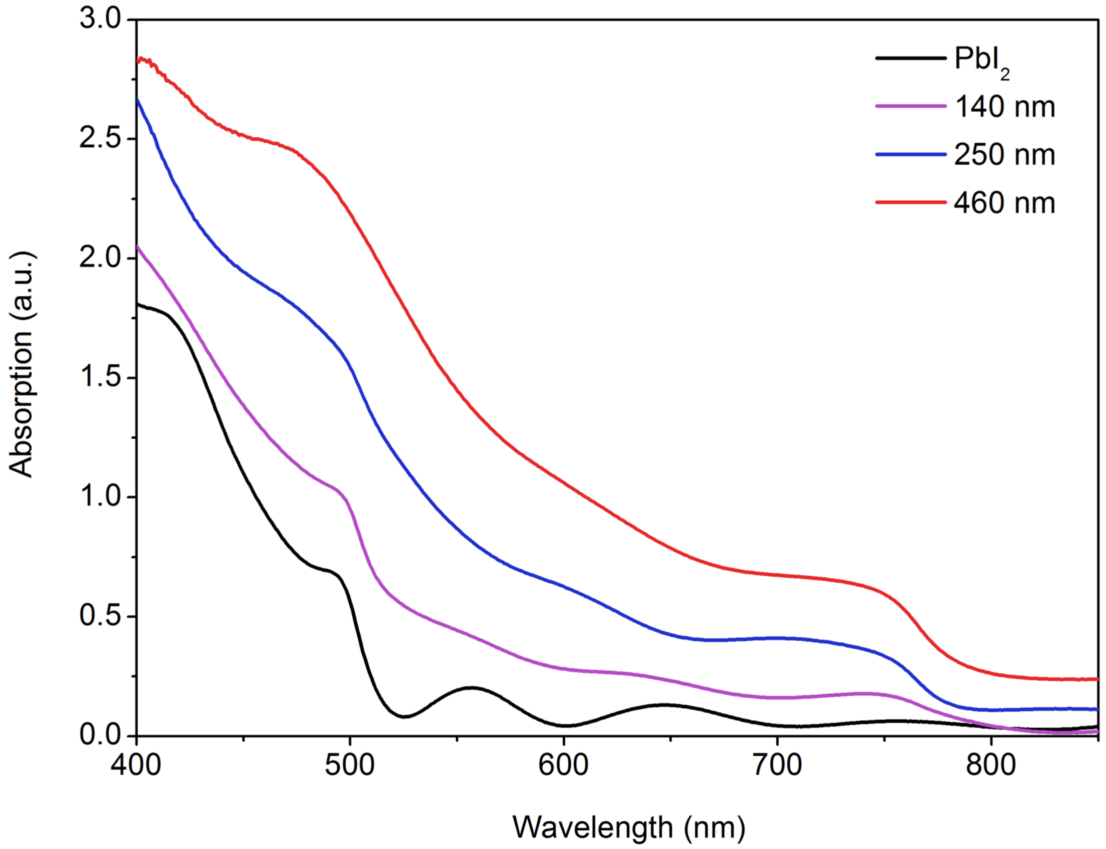

Figure S5. Absoprtion spectra of perovskite $CH_3NH_3PbI_3$ layers with increasing thicknesses.

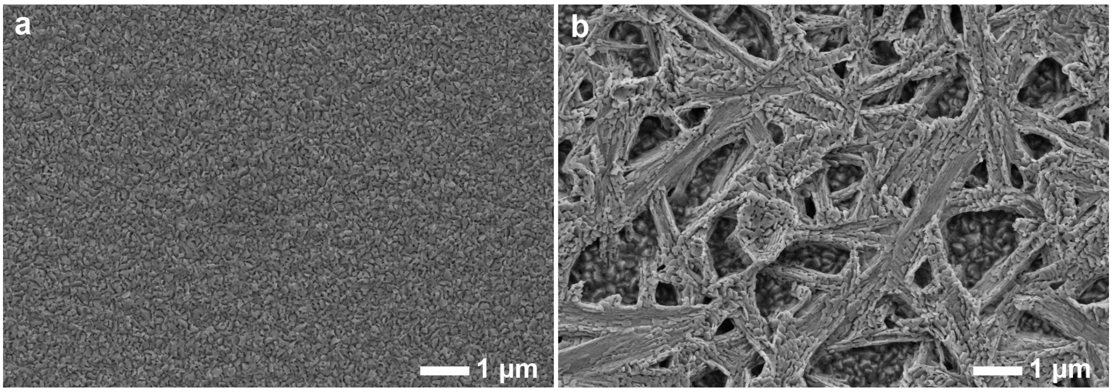

Figure S6. SEM images of PbI_2 layers with thicknesses of 300 nm (**a**) and 800 nm (**b**).

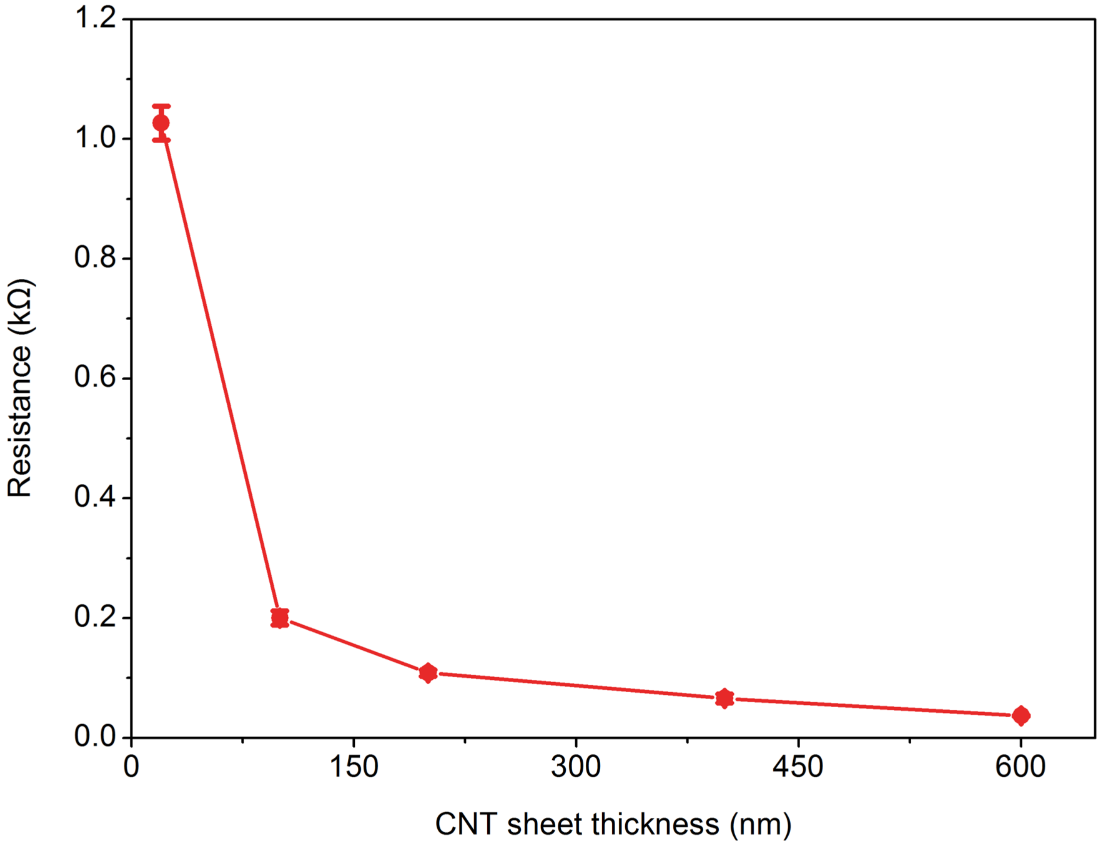

Figure S7. Dependence of electrical resistance on thickness of CNT sheet.

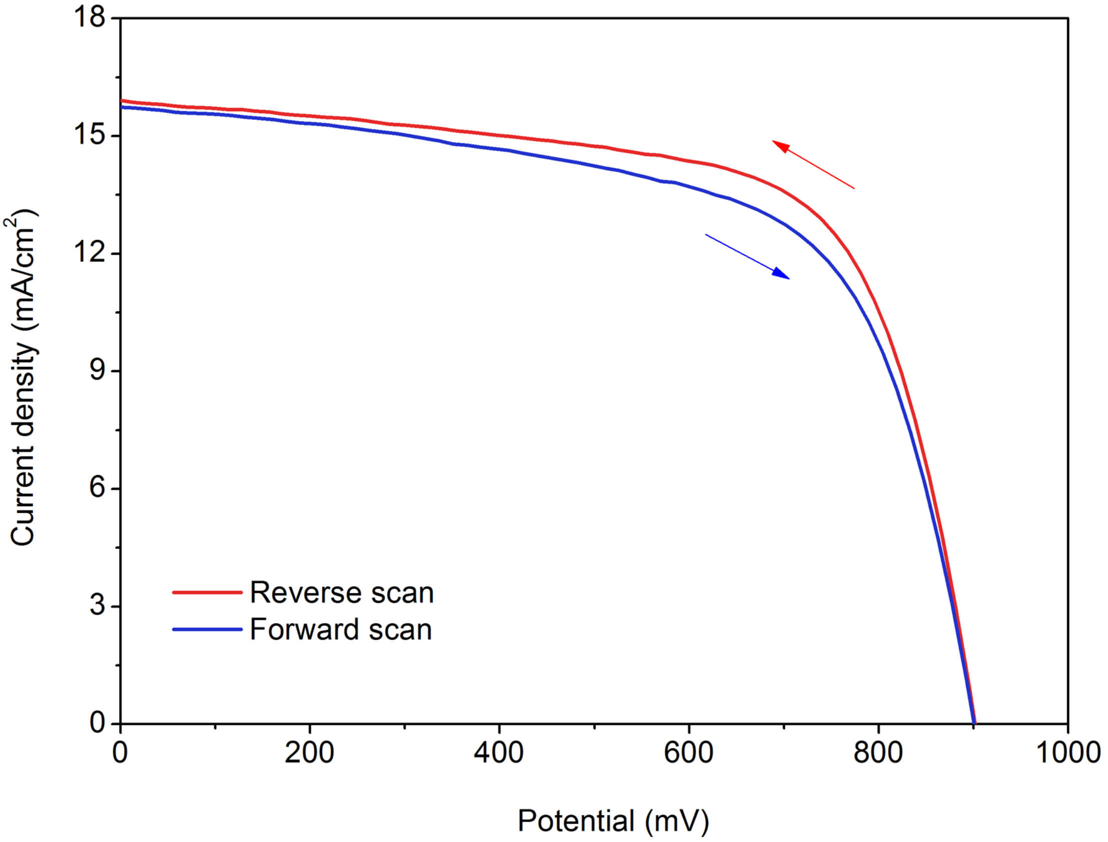

Figure S8. J-V curves of a FPSC under forward and reverse scans with the same scan rate of 100 mV/s.

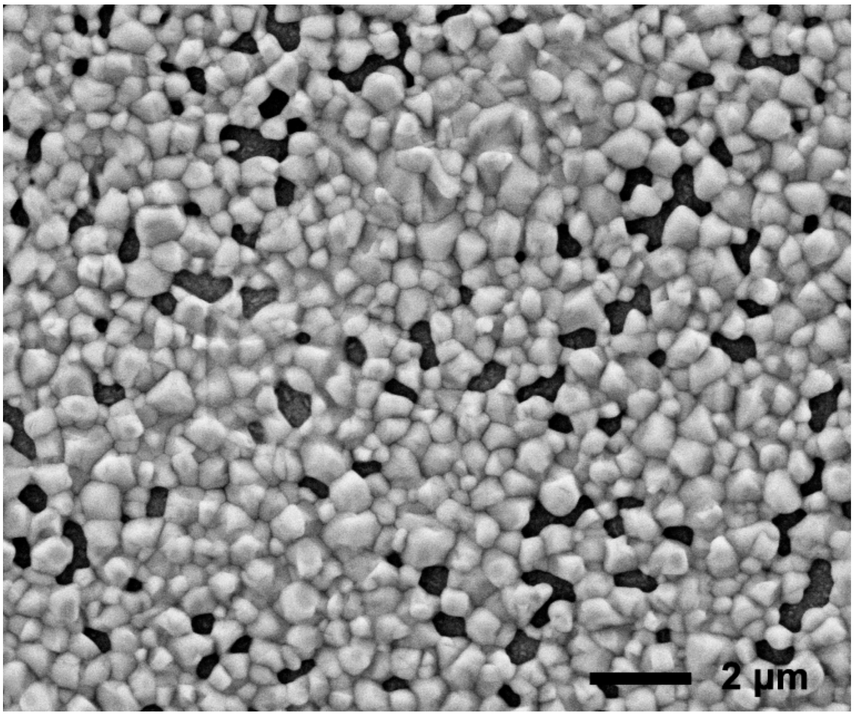

Figure S9. SEM image of perovskite layers on a flat one-dimensional electrode after twisting.

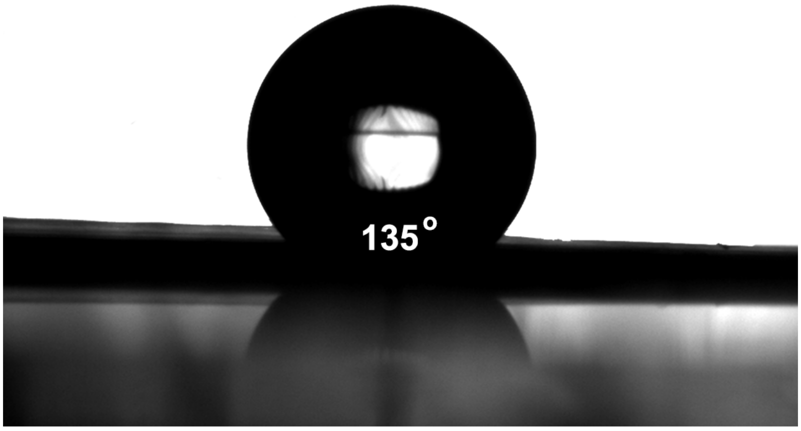

Figure S10. A water droplet on an aligned CNT sheet.